DOI: 10.54254/2755-2721/2026.32371

Disturbance-Observer-Based Tracking Control for a UAV Landing Guidance Platform

Xiaoyu Han

School of Mechatronic Engineering, Changchun University of Science and Technology, Changchun, China

1207077199@qq.com

Abstract. During UAV landing guidance, the electro-optical stabilized tracking platform is required to maintain high line-of-sight (LOS) pointing accuracy. However, in practical engineering environments, disturbances such as wind load, structural friction, and attitude coupling may generate equivalent torque disturbances at the motor shaft, which degrade the tracking performance and even cause significant LOS deviation. To address this problem, this paper proposes a robust control method based on a disturbance observer (DOB). First, a single-axis servo system model with lumped torque disturbance is established based on the dynamic model of a DC torque motor and its load. A three-loop cascade control architecture is adopted, and a disturbance observer based on the nominal inverse model and a Q-filter is embedded in the velocity loop to estimate and compensate disturbances online. The effectiveness of the proposed method is verified through MATLAB simulations. Simulation results show that under step disturbance conditions, the peak LOS error decreases from approximately 0.20 mrad to about 0.18 mrad, demonstrating that the proposed control strategy effectively improves the robustness and disturbance rejection capability of the system.

Keywords: disturbance observer, electro-optical tracking platform, UAV landing guidance, torque disturbance rejection, Q-filter

1. Introduction

With the rapid development of UAV technology, its applications in reconnaissance, inspection, and precision strike have become increasingly widespread. During UAV landing guidance, ground-based electro-optical tracking systems must track targets accurately in real time while laser rangefinders provide distance information between the target and the tracking platform. Conventional servo systems usually employ PI controllers; however, under strong disturbances such as wind load, structural friction, and platform coupling, feedback control alone may be insufficient. Disturbance observer (DOB) techniques have therefore been widely studied to estimate and compensate unknown disturbances [1-3]. Motivated by disturbance suppression requirements in electro-optical tracking platforms, this paper proposes a DOB-based robust tracking control strategy. A single-axis servo model is established and a DOB with a Q-filter is embedded in the velocity loop to estimate

DOI: 10.54254/2755-2721/2026.32371

disturbances online. Simulation results verify the effectiveness of the proposed method, and the LOS pointing accuracy requirement is $\theta_{los,rms} \leq 0.2$ mrad.

2. Single-axis servo system modeling

For disturbance transmission analysis, the single-axis servo system is modeled using the equivalent circuit of the DC torque motor and load in Figure 1. By applying Kirchhoff's voltage law to the armature loop, the electrical equations are obtained as

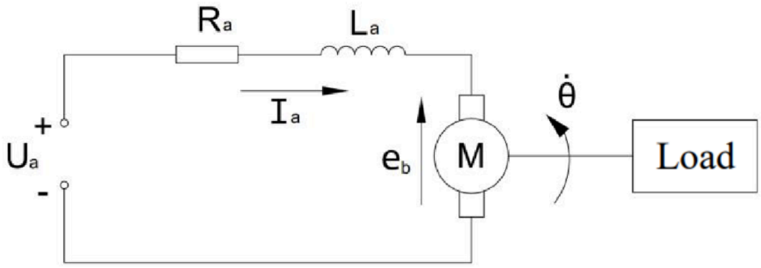

Figure 1. Equivalent circuit of torque motor and load

The corresponding mechanical equation is

$$u_a(t) = R_a i_a(t) + L_a \frac{di_a(t)}{dt} + e_b(t),\ e_b(t) = K_e \dot{\theta}(t),\ M_d(t) = K_m i_a(t) \tag{1}$$

$$J\ddot{\theta}(t) = M_d(t) - M_f(t) \tag{2}$$

where $M_f(t)$ is the lumped disturbance torque accounting for external perturbations acting on the servo system. After taking the Laplace transform, the above equations become.

Applying the Laplace transform to the above equations yields

$$\begin{gathered} U_a(s) = R_a I_a(s) + L_a s I_a(s) + E_b(s) \\ E_b(s) = K_e s\theta(s) \\ M_d(s) = K_m I_a(s) \\ M_d(s) = Js^2\theta(s) + M_f(s) \end{gathered} \tag{3}$$

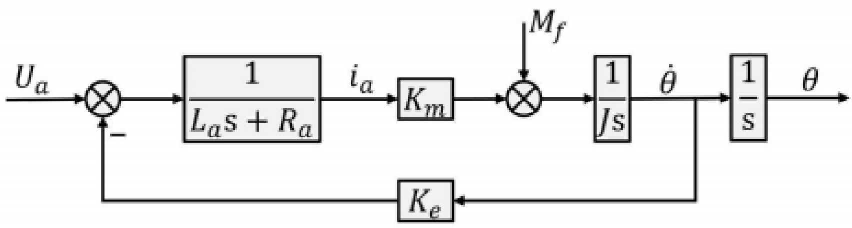

Figure 2. Block diagram of DC torque motor system

If the armature inductance is neglected, or equivalently treated by the time-constant approximation, the motor can be described by the reduced-order form in Figure 2, which is convenient for closed-loop controller design and frequency-domain analysis. Accordingly, the motor electrical and mechanical time constants are given by $T_e = L_a/R_a$ and $T_m = R_a J/(K_e K_m)$, respectively.

DOI: 10.54254/2755-2721/2026.32371

Considering the transfer channel from the control voltage U_a to the angular velocity $\dot{\theta}$ and assuming $M_f = 0$, the transfer function can be written as $\dot{\theta}(s)/U_a(s) = (1/K_e)/[(T_e s+1)(T_m s+1)]$,where $T_e=L_a/R_a$ and $T_m=R_a J/(K_e K_m)$. Since $T_e \ll T_m$, the system can be approximated as a cascade of two first-order dynamics.

3. Controller design

3.1. Control structure

To enable the tracking system to quickly capture and track targets over a wide range, a three-loop cascade control structure is adopted in this paper. Meanwhile, considering practical engineering implementation and parameter tuning, PI controllers are employed. This work mainly focuses on the control strategy of the azimuth axis. In practical engineering systems, the motion range of the elevation axis is much smaller than that of the azimuth axis, and its rotational inertia is also smaller. Therefore, if the controller designed for the azimuth axis meets the performance requirements, the elevation axis can usually meet the requirements as well. A typical three-loop cascade control structure is illustrated in Figure 3.

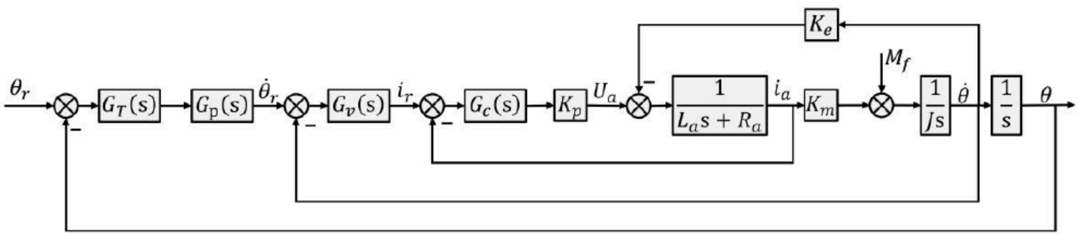

Figure 3. Three-loop servo control structure

The transfer function of the plant can be expressed as

$$G_p(s) = \frac{\theta(s)}{U_a(s)} = \frac{K_m}{JL_a s^3 + JR_a s^2 + K_m K_e s} \tag{4}$$

3.2. Disturbance observer design

The disturbance observer (DOB) is an effective method for disturbance rejection in motion control systems. It was first proposed by Ohnishi in 1987 [4]. The basic idea is to treat disturbances caused by external inputs and model uncertainties as equivalent disturbances acting at the system input and compensate them through the control loop.

Later, Kempf and Kobayashi [5] improved the DOB structure by introducing the inverse of the nominal model instead of the inverse of the actual plant and adding a low-pass Q-filter to ensure robustness. This structure has been widely used in servo systems and industrial motion control applications.

DOI: 10.54254/2755-2721/2026.32371

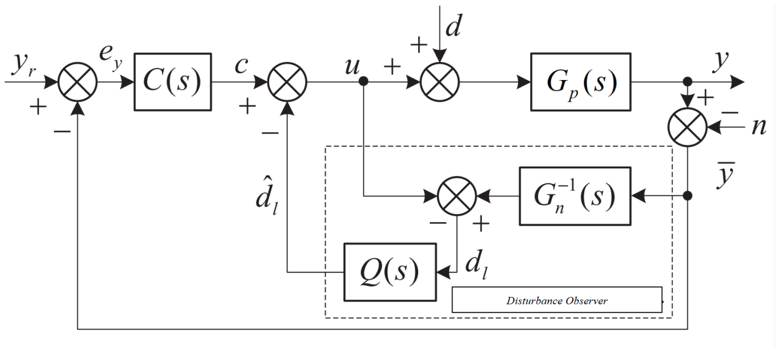

Figure 4. Structure of disturbance observer

Based on the DOB structure shown in Figure 4, the system output can be expressed as

$$y(s) = G_p(s)(u(s) + d(s)) \tag{5}$$

The measured output can be written as

$$\bar{y}(s) = y(s) + n(s) \tag{6}$$

where n(s) represents measurement noise.

3.3. Disturbance estimation

Based on the DOB structure, the disturbance estimate is obtained as

$$\widehat{d}(s) = Q(s)(G_n^{-1}(s)\bar{y}(s) - u(s)) \tag{7}$$

Based on the DOB structure, the disturbance estimate is obtained through the nominal inverse model and the Q-filter. The inverse model reconstructs the nominal plant dynamics, while the Q-filter guarantees robust disturbance estimation and attenuates measurement noise. Similar disturbance estimation mechanisms have been widely adopted in recent disturbance-observer-based control schemes for servo and motion control systems.

3.4. Closed-loop relationship

With disturbance compensation, the system output becomes

$$y(s) = G_p(s)(u(s) - \widehat{d}(s) + d(s)) \tag{8}$$

This expression indicates that the disturbance effect is attenuated by the inner-loop gain GQG_n^{-1}.
When Q(s) approaches unity in the low-frequency range, the disturbance channel is significantly suppressed, resulting in improved tracking accuracy.
Substituting the disturbance estimate leads to

$$y(s) = \frac{G_p(s)(1+Q(s))}{1+G_p(s)Q(s)G_n^{-1}(s)}\,u(s) + \frac{G_p(s)}{1+G_p(s)Q(s)G_n^{-1}(s)}\,d(s) \tag{9}$$

This expression shows that the disturbance effect is attenuated by the inner-loop gain GQG_n^{-1}.

DOI: 10.54254/2755-2721/2026.32371

3.5. Robust stability analysis

Considering modeling errors, the plant can be expressed using multiplicative uncertainty

$$G_p(s) = G_n(s)(1 + \Delta(s)) \tag{10}$$

Where Δ(s) represents model uncertainty.

The robust stability condition can be written as $\|\Delta(j\omega)Q(j\omega)\|_\infty < 1$.

This condition indicates that the Q-filter must attenuate the frequency range where model uncertainty is significant. Therefore, the Q-filter must be carefully designed to guarantee sufficient attenuation in frequency regions where modeling uncertainty is significant.

3.6. Q-filter design

The Q-filter determines the disturbance estimation bandwidth and plays a crucial role in the DOB system. In general, the Q-filter should satisfy two requirements: Q(s) ≈ 1 in the low-frequency region to ensure accurate disturbance estimation, and Q(s) → 0 in the high-frequency region to attenuate measurement noise.

In this study, a second-order low-pass filter is adopted

$$Q(s) = \frac{1}{(\tau s+1)^2} \tag{11}$$

The time constant is selected as τ = 0.001.

This selection provides a trade-off between disturbance rejection and noise suppression.

4. Simulation experiments and result discussion

4.1. Bandwidth preservation check

The disturbance observer may introduce phase lag and affect closed-loop bandwidth. Therefore, the Bode diagrams of the system with and without DOB are compared in Figure 5.

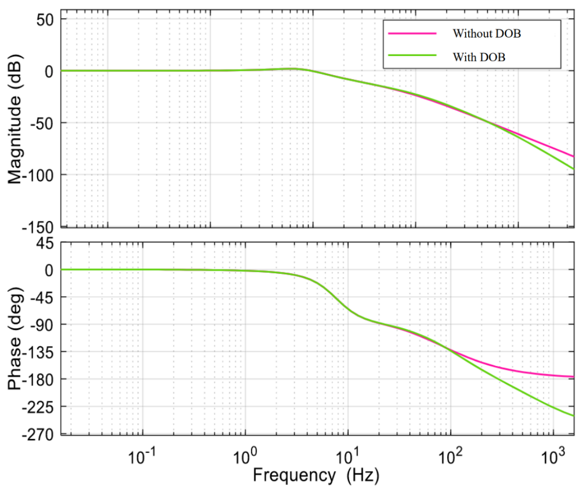

Figure 5. Bandwidth comparison with and without DOB

Figure 5 presents the Bode diagrams of the closed-loop system. It can be observed that the magnitude curves almost overlap in the low-frequency region, and the −3 dB crossover frequency changes only slightly. This indicates that the introduction of the DOB mainly modifies the disturbance channel rather than the reference tracking channel. Consequently, the disturbance rejection capability is improved without sacrificing the system bandwidth. 4.2 Disturbance Rejection Performance

To evaluate the disturbance rejection capability of the proposed controller, three typical torque disturbances are considered: step disturbance, periodic disturbance, and random disturbance.

To evaluate the disturbance rejection capability of the proposed controller, three typical disturbances are considered: step, periodic, and random torque disturbances. Figure 6 presents the tracking errors under these conditions. The peak tracking error without DOB is approximately 0.20 mrad, which decreases to about 0.18 mrad when the DOB is applied. Moreover, the periodic and random disturbance responses show reduced oscillation amplitude without noticeable bandwidth increase, indicating that the Q-filter effectively suppresses disturbances while preventing high-frequency noise amplification.

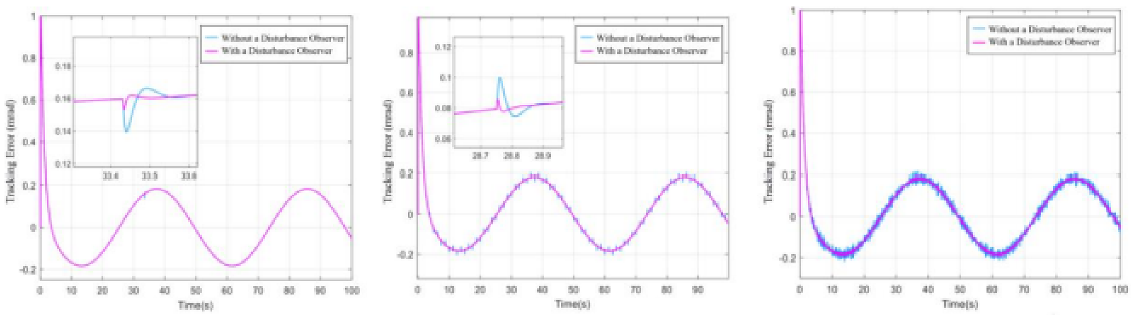

(a) (b) (c)

Figure 6. Tracking errors under different torque disturbances: (a) Step disturbance (b) Periodic disturbance (c) Random disturbance

5. Conclusion

A single-axis EO servo model with lumped torque disturbance was derived and a velocity-loop-embedded DOB was developed within a three-loop cascade architecture. With a realizable and robustly tuned Q-filter, simulations verify notable error suppression under step, periodic and random disturbances while preserving bandwidth. Future work will extend the proposed error-budget and DOB framework to multi-axis coupling compensation and delay-aware prediction in the full landing-guidance system.

References

[1] W. Chen, J. Yang, and L. Guo, "Disturbance-observer-based control and related methods—An overview, " IEEE Transactions on Industrial Electronics, vol. 67, no. 12, pp. 10844–10855, 2020.

[2] S. Li, J. Yang, and W. H. Chen, "Disturbance observer based control for servo systems: A review, " Control Engineering Practice, vol. 107, 104680, 2021.

[3] H. Wang, X. Zhang, and J. Li, "Robust tracking control for UAV electro-optical stabilized platforms under disturbances, " Aerospace Science and Technology, vol. 124, 107487, 2022.

[4] K. Ohnishi, "A new servo method in mechatronics, " Transactions of the Japanese Society of Electrical Engineers, vol. 107-D, no. 1, pp. 83–86, 1987.

DOI: 10.54254/2755-2721/2026.32371

[5] C. J. Kempf and S. Kobayashi, "Disturbance observer and feedforward design for a high-speed direct-drive positioning table, " IEEE Transactions on Control Systems Technology, vol. 7, no. 5, pp. 513–526, 1999.